JOURNAL OF AGRICULTURAL AND FOOD CHEMISTRY

ARTICLE

pubs.acs.org/JAFC

Preparative Separation and Purification of Rebaudioside A from Steviol Glycosides Using Mixed-Mode Macroporous Adsorption Resins

Yongfeng Liu,[†,‡] Duolong Di,[*,†] Qingqing Bai,[§] Jintian Li,[§] Zhenbin Chen,[†,∥] Song Lou,[†,‡] and Helin Ye[†,‡]

[†]Key Laboratory of Chemistry of Northwestern Plant Resources and Key Laboratory for Natural Medicine of Gansu Province, Lanzhou Institute of Chemical Physics, Chinese Academy of Sciences, No. 18 Tianshui Middle Road, Lanzhou 730000, China

[‡]Graduate University of the Chinese Academy of Sciences, No. 19A Yuquan Road, Beijing 100049, China

[§]Department of Pharmacy, Gansu College of Traditional Chinese Medicine, No. 35 Dingxi East Road, Lanzhou 730000, China

[∥]School of Material Science and Engineering, Lanzhou University of Technology, No. 287 Langongping Road, Lanzhou 730050, China

ABSTRACT: Preparative separation and purification of rebaudioside A from steviol glycosides using mixed-mode macroporous adsorption resins (MARs) were systematically investigated. Mixed-mode MARs were prepared by a physical blending method. By evaluation of the adsorption/desorption ratio and adsorption/desorption capacity of mixed-mode MARs with different proportions toward RA and ST, the mixed-mode MAR 18 was chosen as the optimum strategy. On the basis of the static tests, it was found that the experimental data fitted best to the pseudosecond-order kinetics and Temkin−Pyzhev isotherm. Furthermore, the dynamic adsorption/desorption experiments were performed on the mini column packed with mixed-mode MAR 18. After one run treatment, the purity of rebaudioside A in purified product increased from 40.77 to 60.53%, with a yield rate of 38.73% (*W*/*W*), and that in residual product decreased from 40.77 to 36.17%, with a recovery yield of 57.61% (*W*/*W*). The total recovery yield reached 96.34% (*W*/*W*). The results showed that this method could be utilized in large-scale production of rebaudioside A from steviol glycosides in industry.

KEYWORDS: Rebaudioside A, mixed-mode macroporous adsorption resin, steviol glycoside, adsorption kinetics, adsorption isotherms, purification

INTRODUCTION

Steviol glycosides (SGs) are mainly extracted from the leaves of *Stevia rebaudiana* Bertoni, which is native to certain regions of South America (Paraguay and Brazil). SGs, approximately 250−300 times sweeter than sucrose, are white, odorless, and crystalline.[1] To date, previous researches have revealed that SGs mainly contain 10 kinds of diterpenoids, in which stevioside (ST), rebaudioside A (RA), and rebaudioside C (RC) are the predominant sweetening ingredients. The chemical structures of three components are shown in Figure 1.[2] In recent years, because of high sweetness, low calorie, non-nutritive, high stability,[3−6] and many biological effects on humans (such as the treatment of diabetes, antihypertensive, anti-inflammatory, and anticancer effects, and immunomodulatory activities),[7−12] SGs have received great attention and been widely used in foods and beverages in Japan, Korea, China, and South America.[13]

SGs are comprised of various diterpenoids among which ST and RC exhibit after-taste bitterness, thus restricting their use for human consumption and application in food and pharmaceutical products.[14] Consequently, as SGs are added in foods and beverages as additives, the taste will not be easily accepted by the consumer. Furthermore, questions on specifications, safety, and special population (children and consumers with diabetes) effects prevent SGs from obtaining a legal status, permitting their use as a sweetener in most countries.[13] As compared with other compositions in SGs, RA has superior taste quality and thus has been widely applied in the beverage and food industry as an additive in

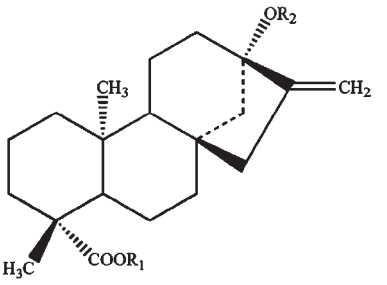

No.	Compound name	R_1	R_2
1	stevioside (ST)	β-Glc	β-Glc-β-Glc(2→1)
2	rebaudioside A (RA)	β-Glc	β-Glc-β-Glc(2→1) β-Glc(3→1)
3	rebaudioside C (RC)	β-Glc	β-Glc-α-Rha(2→1) β-Glc(3→1)

Figure 1. Chemical structures of ST, RA, and RC.

recent decades. Research clearly indicated that RA produced no clinically important changes in blood pressure[15] and was not genotoxic at the doses tested.[16] Specifically, studies on the general and reproductive toxicity of RA demonstrated that it

Received: May 20, 2011
Accepted: July 29, 2011
Revised: July 27, 2011
Published: July 29, 2011

ACS Publications © 2011 American Chemical Society

dx.doi.org/10.1021/jf2020232 | *J. Agric. Food Chem.* 2011, 59, 9629–9636

Table 1. Physical Properties and Moisture Contents of MARs Used

resin series	polarity	structure	particle size (mm)	specific surface area (m^2/g)	pore size (nm)	moisture content (%)
HPD750	middle	SDVB[a]	0.3−1.2	650−700	8.5−9	56.73
LSA-40	middle	SDVB	0.315−1.25	700	7.24	68.28
LX-68M	none	SDVB	0.3	1050	13	60.69
07C	middle	*b*	0.3−1.25	≥350	8.7	68.43

[a] SDVB is the abbreviation of styrene divinyl-benzene. [b] Means not to be collected.

was safe for humans at high dietary intake levels (less than 2 mg/kg body weight per day),[17−19] and ST and RA did not influence significantly the human intestinal microflora composition.[20] The U.S. FDA stated that RA from the leaves of *S. rebaudiana* Bertoni could be considered generally recognized as safe in December 2008. Overall, RA with high purity as a general purpose sweetener is safe for humans under its intended conditions of use.

Because of the significances mentioned above, various technologies of separation and purification for RA with high purity from SGs have been reported. Jackson et al. developed a method for isolating and purifying RA based on the attributes of a given batch of SGs in different solvents.[21] Recently, a series of patents of crystallization and recrystallization for RA were authorized by the U.S. patent office.[22−24] However, these methods exhibit some disadvantages such as tedious process, time and labor consumption, solvent residue (methane et al.), and low efficiency. Therefore, it is crucial to develop a new technology for preparing RA with high purity.

It is known that macroporous adsorption resins (MARs) exhibit many special advantages such simple operation process, low operation cost, little solvent consumption, high efficiency, easy regeneration, long lifetime, and environmental friendliness. Therefore, the method of employing MARs to separate bioactive components from crude extracts of herbal raw materials has attracted increasing attention.[25−28] MARs also played an important role in the preparation of SGs from the leaves of *S. rebaudiana* Bertoni in industry.[29] However, a single component in SGs could not be obtained, depending on the inherent properties of used MAR and analytes of similar chemical structure.

Because of the high separation selectivity and product quality, as well as the high production efficiency in industrial-scale manufacturing, mixed-mode resin separation technologies have been widely applied in the separation and purification fields to purify biological samples.[30−32] To date, there are no reports on using mixed-mode MARs to separate and enrich bioactive components from crude extracts of herbal raw materials and investigate the adsorption/desorption performances. On the basis of the previous works of MARs in our laboratory,[28,33,34] preparative separation and purification RA from SGs by mixed-mode MARs were systematically studied.

MATERIALS AND METHODS

Adsorbents, Samples, and Standards. MARs including HPD750 and 07C were purchased from Cangzhou Bon Adsorber Technology Co., Ltd. (Hebei, China) and Cangzhou Yuanwei Chemical Industry Co., Ltd. (Hebei, China), respectively; LSA-40 and LX-68M were from Xi'an Sunresin Technology Co., Ltd. (Shaanxi, China). The physical and chemical properties of MARs were provided by manufacturers and are summarized in Table 1. SGs (purity >90%) were obtained from Jiuquan Wenming Steviol Glycosides Co., Ltd. (Gansu, China). The standards RA and ST were isolated and purified from SGs by HSCCC in our laboratory.[34] By high-performance liquid chromatography (HPLC)−diode array detection analysis based on the peak area normalization method, the purities of RA and ST were determined as more than 98.5 and 98.3%, respectively. The standards were identified by various spectroscopic methods including ^{1}H NMR, ^{13}C NMR, and distortionless enhancement by polarization transfer−NMR techniques and reference data.

HPLC Analysis of RA and ST. The HPLC analysis was performed in an Agilent 1200 Series (Agilent Technology, United States), and this apparatus was equipped with a G1312A binary pump, a G1315B diode array detector, and a G1328B manual injector. The HPLC system was managed by Agilent Chemstation software (version A.10.02) (Agilent Technology). The standards of RA and ST were accurately weighed and dissolved in ethanol−water (70:30, v/v) to produce the stock standard solutions with the concentrations of 451.5 and 435.5 μg/mL, respectively. The chromatographic separation of analytes was performed on a Hypersil NH_2 column (150 mm × 4.6 mm, i.d., 5 μm) (Dalian Elite Analytical Instruments Co. Ltd., Dalian, China). The temperature of column was maintained at 298.15 K. The mobile phase was acetonitrile−water (80:20, v/v). The flow rate, injection volume, and detect wavelength were set at 1.2 mL/min, 20 μL, and 210 nm,[29,34,35] respectively. The HPLC results demonstrated that the working calibration curve showed excellent linearity over the range of 4.515−451.5 and 4.355−435.5 μg/mL, respectively. The regression lines for RA and ST were $y = 3.0808x - 2.2090$ ($R^2 = 0.9999$, $n = 7$) and $y = 3.6415x + 3.6851$ ($R^2 = 0.9998$, $n = 7$), respectively, where y is the peak area of RA or ST and x is RA or ST concentration (μg/mL).

Mixed-Mode MARs Screening. To screen optimum proportion of mixed-mode MARs for RA separation from the SGs, the adsorption/desorption properties of mixed-mode MARs with different proportions were characterized. First, four kinds of pretreated hydrated MARs (equal to 1 g of dry resins) with a certain proportion and 50 mL of SGs solution were added into a 250 mL stoppered conical flask and shaken in SHA-B incubator (100 rpm) at 318.15 K for 5 h. After the adsorption process reached equilibrium, the raffinate was analyzed by HPLC. Second, the raffinates were removed, and 50 mL of ethanol−water (70:30, v/v) was added into each flask to desorb the corresponding adsorbate loaded mixed-mode MARs. The conical flasks were shaken (100 rpm) at 318.15 K for 2 h, and then, corresponding eluents were analyzed by HPLC. The adsorption/desorption ratio and adsorption/desorption capacity of mixed-mode MARs with different proportions toward RA and ST were evaluated by following equations:

Adsorption ratio:

$$A\,(\%) = \frac{(C_0 - C_e)}{C_0} \times 100\% \quad (1)$$

Desorption ratio:

$$D\,(\%) = C_d \times \frac{V_d}{(C_0 - C_e)V_a} \times 100\% \quad (2)$$

Adsorption capacity:

$$q_e = (C_0 - C_e) \times \frac{V_a}{\sum_{i=1}^{4}(1 - M_i)W_i} \quad (3)$$

dx.doi.org/10.1021/jf2020232 |J. Agric. Food Chem. 2011, 59, 9629–9636

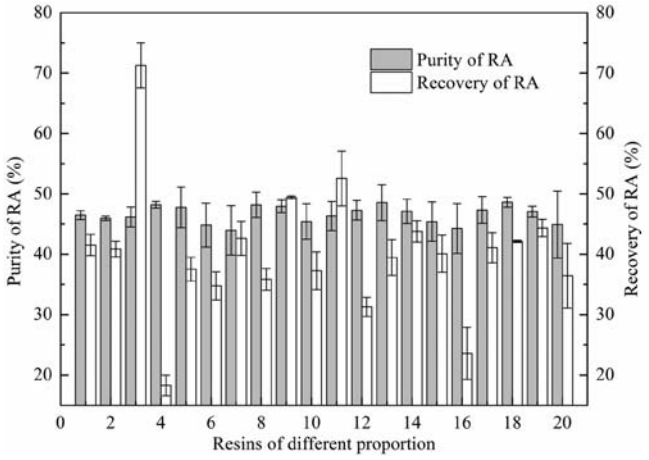

Figure 2. Purity and recovery of RA in effluent solutions after adsorption by mixed-mode MARs with different proportions at 318.15 K. The number in the *X*-axis represented different kinds of resins: 1, HPD750; 2, LSA-40; 3, 07C; 4, LX-68M; 5, 3:1:2:3; 6, 3:3:1:2; 7, 2:1:4:2; 8, 2:1:2:4; 9, 1:2:4:2; 10, 4:2:1:2; 11, 1:2:5:1; 12, 1:1:2:5; 13, 1:5:1:2; 14, 5:1:2:1; 15, 1:6:1:1; 16, 1:1:1:6; 17, 3:2:2:2; 18, 2:3:2:2; 19, 2:2:3:2; and 20, 2:2:2:3 (5−20, a series of mixed-mode MARs with different proportions of HPD750:LSA-40:07C:LX-68M in weight).

Desorption capacity:

$$q_d = C_d \times \frac{V_d}{\sum_{i=1}^{4}(1 - M_i)W_i} \quad (4)$$

where A, D, q_e, and q_d are the adsorption/desorption ratios (%) and capacities (g/g dry resin) toward RA or ST at adsorption/desorption equilibrium, respectively. C_0 and C_e are the initial and equilibrium concentrations of RA or ST solutions (g/L). C_d and V_d are the concentration (g/L) and volume (L) of the desorption solution of RA or ST. V_a is the volume of RA or ST solution used in the study (L). M_i is the moisture content of i kind of resin (%). W_i is the weight of i kind of resin used (g).

Adsorption Kinetics. The adsorption kinetics of RA and ST on the optimum mixed-mode MAR were investigated on the basis of the following operation mode: Pretreated mixed-mode MAR 18 and 50 mL of SGs solution were added into a 250 mL stoppered conical flask and shaken at 318.15 K. Then, the raffinates at different time intervals from start to equilibration were analyzed by HPLC.

Adsorption Isotherm and Thermodynamics. SGs solutions (50 mL) with different concentrations of RA and ST were contacted with pretreated mixed-mode MAR 18 in conical flasks, continually shaken for 5 h at temperatures of 298.15, 308.15, and 318.15 K, respectively. Then, the raffinates were analyzed by HPLC.

Dynamic Adsorption/Desorption Experiments on Mini Column. Dynamic adsorption/desorption tests were performed in a glass column (1.3 cm × 40 cm) packed with mixed-mode MAR 18 with a bed volume (BV) of 10 mL. The adsorption process was performed as follows: The SGs solution was loaded onto the pretreated glass column and then performed adsorption onto the mixed-mode MAR 18. The raffinate was analyzed by HPLC. The adsorbate-laden column was desorbed with ethanol−water (70:30, v/v). Furthermore, the eluent was analyzed by HPLC. The concentration of RA, flow rate, ratio of diameter to height in the adsorption process, and volume and flow rate of eluent in desorption process at 318.15 K were systematically investigated.

RESULTS AND DISCUSSION

Adsorption Characteristics of Mixed-Mode MARs with Different Proportions. The adsorption characteristics of mixed-mode MARs with different proportions were obtained through static adsorption/desorption experiments at 318.15 K, and the results are shown in Figure 2. It can be seen that the purity of RA was in the order of LSA-40 < 07C < HPD750 < LX-68M. The molecular structures of ST, RA, and RC are shown in Figure 1, and it was obviously seen that the molecular size of ST was smaller than that of RA. The physical properties of MARs are shown in Table 1, and it was clear that the pore size of four MARs was in the order of LSA-40 < 07C < HPD750 < LX-68M. Therefore, it indicated that the larger the pore size was, the higher the purity of RA was. In other words, the effect of molecular size for target compounds on diffusion into micropore of MARs was crucial. Thus, as compared with RA, ST was easily diffused into micropore of MARs. Accordingly, the purity of RA was higher in the raffinate after adsorption. In brief, molecular sieving effect was the dominating factor in the enrichment process of RA.

From Figure 2, the recovery of RA followed an order of 07C > HPD750 > LSA-40 > LX-68M. In terms of specific surface areas of MARs, it followed an order of 07C < HPD750 < LSA-40 < LX-68M as shown in Table 1. It meant that the higher the specific surface area was, the lower the recovery of RA was. Thus, the specific surface area was the main factor for the recovery of RA. All in all, the matching of the pore size of the adsorbent with the size of the adsorbate and suitable specific surface areas of MARs were considered to be the predominant factors affecting separation.

However, the ideal purity and recovery of RA could not be simultaneously obtained using single MAR. For this reason, mixed-mode MARs with different proportions were screened to separate RA from the SGs. In Figure 2, it could be found that the higher purity and recovery of RA might be obtained on mixed-mode MAR 18, which meant that molecular sieving and specific surface area effects between the adsorbent and the adsorbate could be perfectly coordinated. Therefore, the mixed-mode MAR 18 was selected for further investigation.

Adsorption/Desorption Kinetics on the Mixed-Mode MAR 18. Adsorption kinetics curves of RA and ST on mixed-mode MAR 18 were obtained at 318.15 K, as shown in Figure 3A. In general, the adsorption capacity increased rapidly in the first 1 h due to rapid attachment of RA to the macropore of mixed-mode MAR 18 and then increased slowly because of diffusion of RA from macropore into the mesopore/micropore of the mixed-mode MAR 18. Finally, the adsorption capacity reached equilibrium after 4 h. In short, the adsorption capacity of RA on mixed-mode MAR 18 increased with the extension of adsorption time until equilibrium. The adsorption process of ST was the same as that of RA. The adsorption processes of RA and ST reached equilibrium at around 4 h, and the result indicated that the mixed-mode MAR 18 pertained to the slow adsorption type (fast adsorption, t_a < 2 h; intermediate speed adsorption, 2 h < t_a < 3 h; and slow adsorption, t_a > 3 h). Therefore, for the purpose of complete adsorption, the adsorption time was set mainly over 4 h. The slow adsorption was caused by the following reasons: As shown in Figure 1, RA and ST exhibit the structure of diterpenoid glucoside, and thus, corresponding molecular sizes are much larger than flavonoids. In addition, the pore sizes of mixed-mode MAR 18 are heterogeneous. Hence, high intraparticle mass transfer resistance existed in the process of RA and ST diffusing into the micropore of the mixed-mode MAR 18. Furthermore,

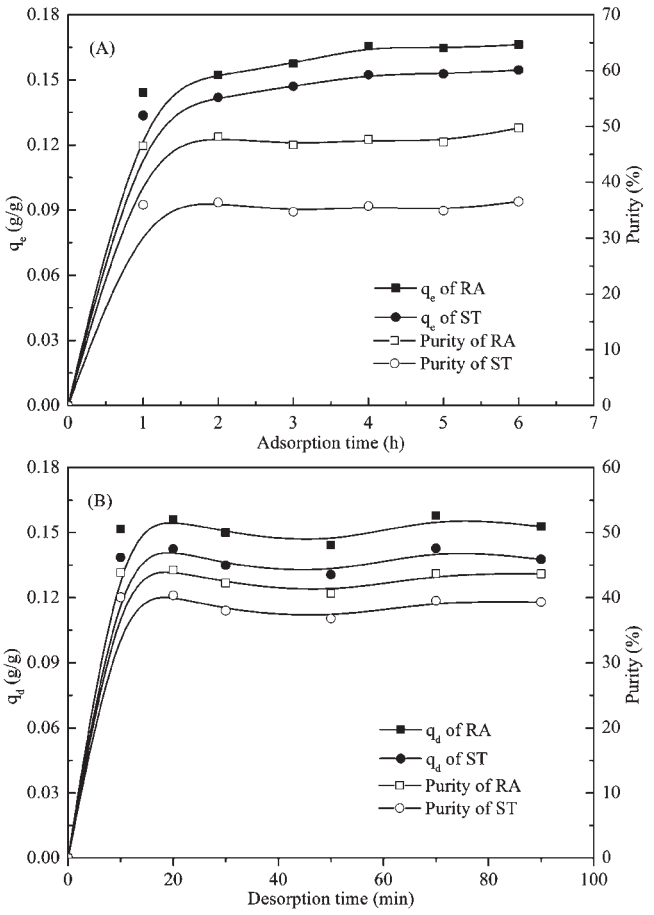

Figure 3. Adsorption (A) and desorption (B) kinetics curves of RA and ST on mixed-mode MAR 18 at 318.15 K.

from the standpoint of the purity of effluent solution, the adsorption processes of RA and ST reached equilibrium after 2 h (Figure 3A), which meant that the proportion of RA and ST in effluent solution remained unchanged after 2 h.

To better understand the enrichment mechanism of RA, the following kinetic models, pseudofirst-order, pseudosecond-order, Elovich equation, and intraparticle diffusion kinetics, were used to fit the experimental data.

The pseudofirst-order kinetic equation:

$$\ln(q_e - q_t) = \ln q_e - k_1 t \quad (5)$$

The pseudosecond-order kinetic equation:

$$t/q_t = 1/k_2 q_e^{\,2} + t/q_e \quad (6)$$

The Elovich equation:

$$q_t = \frac{1}{\beta}\ln(\alpha\beta) + \frac{1}{\beta}\ln t \quad (7)$$

The intraparticle diffusion kinetic equation:

$$q_t = k_{id} t^{1/2} + C \quad (8)$$

where q_e and q_t are the adsorption capacity at equilibrium and at any time t (g/g dry resin), respectively. k_1 (1/min), k_2 [g/(g min)], and k_{id} [g/(g min$^{1/2}$)] are the rate constants of pseudofirst-order, pseudosecond-order, and intraparticle diffusion model, respectively. C (g/g) represents boundary layer thickness. The parameter

Table 2. Kinetics Parameters for the Adsorption Process of RA and ST onto Mixed-Mode MAR 18

	kinetics parameters	
kinetics models	RA	ST
pseudofirst-order equation		
k_1 (1/min)	−0.003662	0.01128
q_e (g/g)	0.006377	0.04495
R^2	0.7790	0.9414
pseudosecond-order equation		
k_2 [g/(g min)]	−0.6538	0.4481
q_e (g/g)	0.1094	0.1602
R^2	0.9995	0.9997
Elovich equation		
α [g/(g min)]	−15.1929	6.9843
β (g/g)	−82.7815	82.7815
R^2	0.9821	0.9821
intraparticle diffusion equation		
k_{id} [g/(g min$^{1/2}$)]	−0.001890	0.001890
C (g/g)	0.1473	0.1206
R^2	0.9430	0.9430

α is the initial adsorption rate [g/(g min)], and β is the desorption constant (g/g).

Plotting $\ln(q_e - q_t)$ against t, t/q_t against t, q_t versus ln t, and q_t versus $t^{1/2}$ would get straight lines, respectively. The calculated results are shown in Table 2. By checking the values of linear regression correlation coefficients, it was found that the pseudosecond-order kinetics provided a good correlation for the adsorption of RA and ST onto the mixed-mode MAR 18. It demonstrated that the concentration of adsorbate was closely related to the rate-determining step in the adsorption process, which might be chemical adsorption.[36] In terms of the rate constants of the kinetic model for the adsorption process of ST, the value of k_2 was positive, which showed that q_e for ST on mixed-mode MAR 18 increased with the extension of adsorption time until equilibrium. However, for the adsorption process of RA, k_2 was a negative value, which demonstrated that it was disadvantageous for the adsorption of RA on mixed-mode MAR 18. In other words, RA adsorbed on the mixed-mode MAR 18 could be replaced by ST in the solution in the whole adsorption process.

Desorption kinetics curves of RA and ST on mixed-mode MAR 18 were also obtained at 318.15 K, which are shown in Figure 3B. It was observed that the desorption capacities for RA and ST remained constants after 20 min, suggesting that desorption was very quick and effective process when ethanol−water (70:30, v/v) was used as an eluent. This phenomenon indicated that the force between mixed-mode MAR 18 and RA or ST was weaker than the force between the eluent and RA or ST. Moreover, the tendency of purity was similar to that of desorption capacity. Thus, desorption processes of RA and ST reached equilibrium after 20 min.

Adsorption Isotherms of RA and ST on Mixed-Mode MAR 18. The equilibrium adsorption isotherms of RA and ST from SGs aqueous solution onto mixed-mode MAR 18 were obtained at 298.15, 308.15, and 318.15 K, respectively, as in Figure 4. It was obvious that the adsorption capacities of RA onto mixed-mode MAR 18 increased with an increase in temperature in

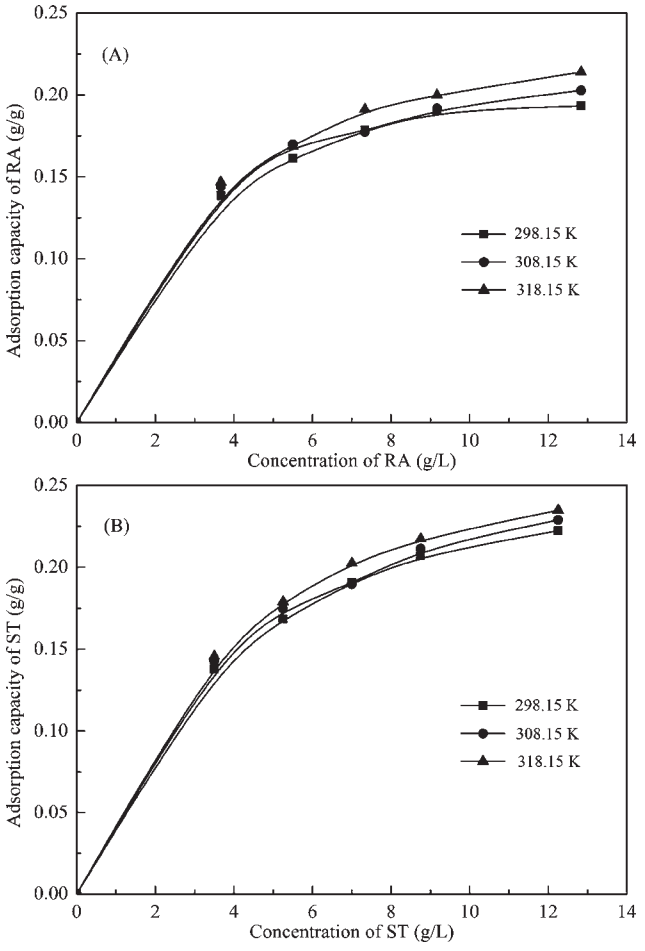

Figure 4. Adsorption isotherms of RA and ST on mixed-mode MAR 18 at different temperatures.

Figure 4A, which might be suggested as an endothermic process. Furthermore, the adsorption capacities of RA also increased as the concentration of solution increased. Generally, the adsorption capacity increased rapidly as the concentration of solution was less than 6 g/L and then increased slowly. A similar result illustrated in Figure 4B was obtained for ST.

The adsorption isotherm is one of the most important approaches to illustrate the mechanism of the adsorption systems. Langmuir, Freundlich, Temkin−Pyzhev, and Dubinin−Radushkevich isotherms were adopted to analyze experimental data.

The Langmuir isotherm equation is represented as:

$$C_e/q_e = K_L/q_m + C_e/q_m \quad (9)$$

The Freundlich isotherm equation is shown as:

$$\lg q_e = (1/n) \lg C_e + \lg K_F \quad (10)$$

The Temkin−Pyzhev isotherm equation[37] is given as:

$$q_e = (RT/b_T) \ln C_e + (RT/b_T) \ln A \quad (11)$$

The Dubinin−Radushkevich isotherm equation[38] is:

$$\ln q_e = -\beta\varepsilon^2 + \ln q_m \quad (12)$$

where q_e and q_m are the equilibrium and maximum adsorption capacity (g/g dry resin), respectively. C_e is the equilibrium concentration of RA or ST solution (g/L). K_L is the parameter related to the adsorption energy (g/L). K_F reflects the adsorption capacity of an adsorbent $[(g/g)(L/g)^{1/n}]$. The parameter n represents the adsorption affinity of the adsorbent for an adsorbate. R is the gas constant [8.314 J/(mol K)]. T is the absolute temperature (K). b_T and A are the Temkin−Pyzhev constant (J/mol) and isotherm constant (L/g), respectively. β is a constant related to the mean free energy of adsorption per mole of an adsorbate (mol^2/J^2), and ε is the Polanyi potential, equal to $RT \ln(1 + 1/C_e)$.

Plotting $1/q_e$ against $1/C_e$, lg q_e versus lg C_e, q_e against ln C_e, and ln q_e versus ε^2, would get straight lines, respectively. The values of corresponding parameters could be calculated from the intercept and slope. The results are shown in Table 3. The specific adsorption mechanisms were narrated in detail in the following discussion.

As shown in Table 3, a good correlation coefficient of Langmuir isotherm was obtained. Consequently, the adsorption mechanism of RA and ST could be deciphered by the Langmuir isotherm theory. A dimensionless separation factor, namely, the equilibrium parameter, R_L, should be considered. The R_L was given as:

$$R_L = \frac{1}{1 + C_0/K_L} \quad (13)$$

where C_0 is the highest initial concentration of RA or ST (g/L) and K_L is the Langmuir constant (g/L). The value of R_L gives an indicator of the shape of isotherm to be either unfavorable ($R_L > 1$), linear ($R_L = 1$), favorable ($0 < R_L < 1$), or irreversible ($R_L = 0$). It was clear as in Table 3 that the R_L values were in the range of $0 < R_L < 1$. Therefore, it was favorable for the adsorption of RA or ST on mixed-mode MAR 18.

The corresponding parameters obtained from Freundlich isotherm equation were tabulated in Table 3. By the comparison of correlation coefficients, it could be seen that the Freundlich isotherm was also a good model for RA or ST adsorption. K_F could be defined as the adsorption or distribution coefficient.[39] Thus, the values of K_F corresponded to the quantity of RA or ST adsorbed onto the mixed-mode MAR 18. According to Freundlich isotherm theory, the value of $1/n$ was a measure of adsorption intensity or surface heterogeneity, and the closer the value got to zero, the more heterogeneous the surface was. The value of $1/n$ below 1 demonstrated normal isotherm, and above 1 was indicative of cooperative adsorption. In Table 3, the values of $1/n$ were ranged from 0 to 1 for RA and ST onto the mixed-mode MAR 18, which indicated a normal isotherm. The values of $1/n$ for RA onto the mixed-mode MAR 18 were smaller than those for ST at the temperatures studied. This meant that the adsorption intensity of RA was larger than that of ST. However, experimental data manifested that the adsorption intensity of ST was larger than that of RA. The reason was that the molecular size of ST was smaller than that of RA, and a small molecular size was advantageous for ST to diffuse into micropore of mixed-mode MAR 18.

The adsorption data were analyzed in accordance with the linear form of Temkin−Pyzhev isotherm equation. The correlation coefficients obtained from Temkin−Pyzhev model were higher than those of Langmuir and Freundlich equations, indicating that the Temkin−Pyzhev isotherm fitted better to RA and ST adsorption data on the mixed-mode MAR 18. The adsorption heats (b_T) were found to be 96.527, 104.655, and

Table 3. Isotherm Parameters for the Adsorption Process of RA and ST onto Mixed-Mode MAR 18 at Different Temperatures

	RA			ST		
isotherm model	298.15 K	308.15 K	318.15 K	298.15 K	308.15 K	318.15 K
Langmuir isotherm						
q_m (g/g)	0.1996	0.2014	0.2118	0.2258	0.2250	0.2343
K_L (g/L)	0.4207	0.3403	0.3675	0.5133	0.4096	0.4057
r_L^2	0.9515	0.9288	0.8903	0.9501	0.9176	0.9450
R_L	0.04467	0.03710	0.04094	0.06147	0.05034	0.05062
Freundlich isotherm						
K_F [(g/g)(L/g)$^{1/n}$]	0.1422	0.1492	0.1523	0.1469	0.1542	0.1606
$1/n$	0.1555	0.1430	0.1621	0.2117	0.1949	0.1964
r_F^2	0.9550	0.9795	0.9838	0.9901	0.9893	0.9922
Temkin−Pyzhev isotherm						
b_T (kJ/mol)	96.527	104.655	91.908	66.332	72.392	72.310
A (g/L)	249.7946	438.6676	196.1080	50.7926	78.6553	82.3644
r_T^2	0.9616	0.9807	0.9813	0.9950	0.9818	0.9978
Dubinin−Radushkevich isotherm						
q_m (mmol/g)	0.1936	0.1974	0.2064	0.2561	0.2593	0.2692
β ($\times 10^{-7}$ mol^2/J^2)	1.0023	0.7982	0.8265	1.3606	1.0726	1.0313
$r_{D\text{-}R}^2$	0.8548	0.8179	0.7594	0.8212	0.7750	0.8194
E (kJ/mol)	2.2335	2.5028	2.4596	1.9170	2.1591	2.2019

91.908 kJ/mol for RA and 66.332, 72.392, and 72.310 kJ/mol for ST at 298.15, 308.15, and 318.15 K, respectively. Therefore, the magnitude of b_T demonstrated that the adsorption of RA and ST from aqueous solution by the mixed-mode MAR 18 was feasible.

For the Dubinin−Radushkevich isotherm, the correlation coefficients were lower than those above-mentioned equations. However, the constant β gives an idea about the mean free energy E (kJ/mol) of adsorption per molecule of an adsorbate from the solution. The parameter E could be calculated from the equation given as:

$$E = 1/\sqrt{2\beta} \tag{14}$$

The value of E gives information that whether adsorption mechanism is ion-exchange or physical adsorption. Hence, it is useful for predicting the type of adsorption process. The adsorption process might be physical adsorption, while E is in the range of 1−8 kJ/mol, and chemical adsorption when E is more than 8 kJ/mol.[38] It could be seen from Table 3, the values of E were found to be 2.2335, 2.5028, and 2.4596 kJ/mol for RA and 1.9170, 2.1591, and 2.2019 kJ/mol for ST at 298.15, 308.15, and 318.15 K, respectively. Therefore, it was possible to say that the types of the adsorption of RA and ST on the mixed-mode MAR 18 were simple physical adsorption.

Adsorption Thermodynamics of RA and ST on Mixed-Mode MAR 18. To account for the adsorption processes of RA and ST on mixed-mode MAR 18, values of thermodynamic parameters were further calculated. The equilibrium constant K (L/mol) was related to the Langmuir isotherm constant (K_L). The free energy of adsorption (ΔG^0) was concerned with the equilibrium constant K. Enthalpy (ΔH^0) and entropy (ΔS^0) changes were calculated based on the Van't Hoff equation. Consequently, ΔG^0, ΔH^0, and ΔS^0 could be estimated by the following equations:

$$K = M/K_L \tag{15}$$

$$\Delta G^0 = -RT \ln K \tag{16}$$

$$\ln K = -\Delta H^0/RT + \Delta S^0/R \tag{17}$$

where M is the molecular weight of RA or ST (g/mol). T is the absolute temperature (K). Plotting ln K as a function of $1/T$ yielded a straight line. The values of ΔH^0 and ΔS^0 were calculated from the slope and intercept of eq 17, respectively.

The ΔG^0 values of adsorption were negative (−2.4711, −2.5540, and −2.6372 kJ/mol for RA and −2.4715, −2.5544, and −2.6375 kJ/mol for ST, respectively) at the temperatures investigated, which suggested that the adsorption processes of RA and ST on mixed-mode MAR 18 were spontaneous. The positive values of ΔH^0 (5.4524 kJ/mol for RA and 9.3651 kJ/mol for ST, accordingly) indicated that the adsorption processes were endothermic. The results were in accordance with the tendency that adsorption capacity increased with the temperature. Furthermore, the absolute values of ΔH^0 were lower than 43 kJ/mol. Therefore, the adsorption processes of RA and ST were physical adsorption. The result corresponded to that derived from the mean free energy E. The positive ΔS^0 values [83.0197 J/(mol K) for RA and 92.8611 J/(mol K) for ST, respectively] implied increasing randomness at the solid−solution interface during the adsorption process.

DYNAMIC ADSORPTION/DESORPTION TESTS ON MINI COLUMN

Effect of Feeding Concentration in Dynamic Adsorption Process. Because the feeding concentration was an important factor in the process of dynamic adsorption, the effect of feeding concentration on adsorption was investigated. For the sake of convenience of investigation, the parameters were kept constant except the one under investigation. As the feeding concentration of RA (9.44, 11.80, 14.16, 16.51, 18.87, and 21.23 g/L) increased,

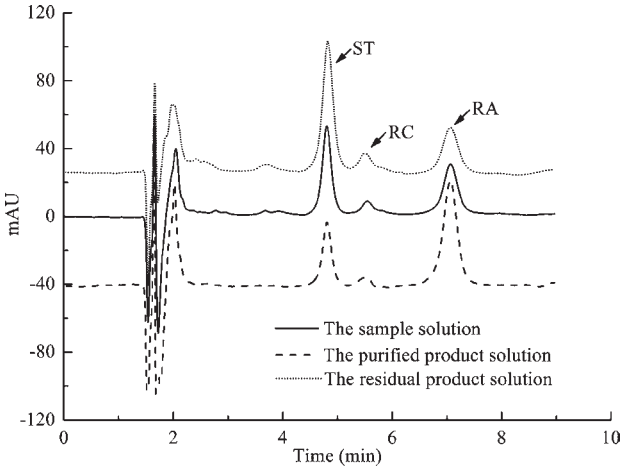

Figure 5. Chromatograms of the sample solutions before and after purification on mixed-mode MAR 18. ST, RC, and RA are the abbreviations of ST, RC, and RA, respectively.

the purity of RA in effluent (59.33, 57.41, 56.17, 54.14, 53.44, and 51.17%) decreased, but the yield rate of RA (11.00, 27.89, 38.18, 44.12, 52.45, and 56.42%) increased. Considering the purity and yield rate of RA, the optimum concentration of RA solution was 14.16 g/L.

Effects of Flow Rate in Dynamic Adsorption Process. The flow rate played an important role in dynamic adsorption process on mini column. Test results showed that as the flow rate (3, 6, and 9 BV/h) increased, the purity of RA in effluent (58.48, 56.17, and 54.62%) decreased, but the yield rate of RA (36.10, 38.18, and 39.09%) increased. Generally speaking, low flow rate endows a positive effect for adsorption process because adsorbate molecules have sufficient time to interact with active sites at the surface of resins and vice versa. Therefore, as the flow rate was low, the contact time between RA molecules and the resin was longer enough to get product with high purity. However, taking the yield rate of RA and time consumption into consideration, the optimum flow rate was set as 6 BV/h.

Effects of Ratio of Diameter to Height in Dynamic Adsorption Process. The bed height is also a significant factor, relative to the theoretical plate number of chromatography theory. It is well-known that the number of the theoretical plate (N) is the major determinant factor for column efficiency. The equation is $N = L/H$, where L is the length of the chromatic column and H is the theoretical plate height. In this study, H was a constant value using mixed-mode MAR 18. Thus, to increase the N value, the only approach was to extend the L value. A series of test results showed that as the ratio of diameter to height (1:10, 1:20, 1:30, 1:40, 1:50, and 1:60) increased, the purity of RA in effluent (54.17, 54.33, 55.64, 56.09, 56.82, and 57.88%) increased, but the yield rate of RA (43.31, 39.90, 37.80, 37.78, 37.38, and 34.02%) decreased. In other words, the increase in bed height was advantageous to the separation of RA from SGs. However, the higher the bed height was, the larger the pressure was. The large pressure made the mixed-mode MAR 18 partly being crushed so that separation efficiency decreased. Therefore, the optimum ratio of diameter to height was set as 1:30.

Dynamic Desorption Tests. After the dynamic adsorption process was absolutely completed at the optimum experimental condition, the adsorbate-laden column was desorbed with ethanol—water (70:30, v/v), and the amount of eluent was 10 BV as the proper volume, while the flow rate was 6 BV/h. The obtained eluent solutions were analyzed by HPLC.

According to the above experiments, the HPLC chromatograms of the sample solutions before and after purification are shown in Figure 5. As compared to the SGs solution, the relative peak area of ST obviously decreased and that of RA significantly increased after purification in the purified product solution, while the relative peak area of ST obviously increased and that of RA significantly decreased after purification in the residual product solution. After one run treatment, the purity of RA in purified product increased from 40.77 to 60.53%, with a yield rate of 38.73% (W/W), and that in residual product decreased from 40.77 to 36.17%, with a recovery yield of 57.61% (W/W). The total recovery yield reached 96.34% (W/W).

As compared to other methods, this method possessed a lower yielding cost, was less labor intensiveness, had more procedural simplicity, and was more environmentally friendly.[40] The results showed that this method could provide help in the development of large-scale production of high-purity RA from SGs in industry. Furthermore, the study may provide scientific references for separating and enriching other bioactive components from crude extracts of herbal raw materials using mixed-mode MARs.

AUTHOR INFORMATION

Corresponding Author

*Tel: +86-931-496-8248. Fax: +86-931-827-7088. E-mail: didl@licp.cas.cn.

Funding Sources

This research project was financially supported by the National Natural Sciences Foundation of China (NSFC No. 20974116) and the "Hundred Talents Program" of the Chinese Academy of Sciences (CAS).

REFERENCES

(1) Soejarto, D.; Compadre, C.; Medon, P.; Kamath, S.; Kinghorn, A. Potential sweetening agents of plant origin. II. field search for sweet-tasting Stevia species. *Econ. Bot.* **1983**, *37* (1), 71–79.

(2) Geuns, J. M. C. Stevioside. *Phytochemistry* **2003**, *64* (5), 913–921.

(3) Clos, J. F.; DuBois, G. E.; Prakash, I. Photostability of Rebaudioside A and Stevioside in Beverages. *J. Agric. Food Chem.* **2008**, *56* (18), 8507–8513.

(4) Wölwer-Rieck, U.; Tomberg, W.; Wawrzun, A. Investigations on the Stability of Stevioside and Rebaudioside A in Soft Drinks. *J. Agric. Food Chem.* **2010**, *58* (23), 12216–12220.

(5) Chang, S. S.; Cook, J. M. Stability studies of stevioside and rebaudioside A in carbonated beverages. *J. Agric. Food Chem.* **1983**, *31* (2), 409–412.

(6) Kroyer, G. Stevioside and Stevia-sweetener in food: application, stability and interaction with food ingredients. *J. Verbraucherschutz Lebensmittelsicherh.* **2010**, *5* (2), 225–229.

(7) Kinghorn, A. D.; Soejarto, D. D. Discovery of terpenoid and phenolic sweeteners from plants. *Pure Appl. Chem.* **2002**, *74* (7), 1169–1179.

(8) Maki, K. C.; Curry, L. L.; Reeves, M. S.; Toth, P. D.; McKenney, J. M.; Farmer, M. V.; Schwartz, S. L.; Lubin, B. C.; Boileau, A. C.; Dicklin, M. R.; Carakostas, M. C.; Tarka, S. M. Chronic consumption of rebaudioside A, a steviol glycoside, in men and women with type 2 diabetes mellitus. *Food Chem. Toxicol.* **2008**, *46* (7, Suppl. 1), S47–S53.

(9) Hsieh, M. H.; Chan, P.; Sue, Y. M.; Liu, J. C.; Liang, T. H.; Huang, T. Y.; Tomlinson, B.; Chow, M. S. S.; Kao, P. F.; Chen, Y. J. Efficacy and tolerability of oral stevioside in patients with mild essential

hypertension: A two-year, randomized, placebo-controlled study. *Clin. Ther.* **2003**, *25* (11), 2797–2808.

(10) Yasukawa, K.; Kitanaka, S.; Seo, S. Inhibitory Effect of Stevioside on Tumor Promotion by 12-*O*-Tetradecanoylphorbol-13-acetate in Two-Stage Carcinogenesis in Mouse Skin. *Biol. Pharm. Bull.* **2002**, *25* (11), 1488–1490.

(11) Mizushina, Y.; Akihisa, T.; Ukiya, M.; Hamasaki, Y.; Murakami-Nakai, C.; Kuriyama, I.; Takeuchi, T.; Sugawara, F.; Yoshida, H. Structural analysis of isosteviol and related compounds as DNA polymerase and DNA topoisomerase inhibitors. *Life Sci.* **2005**, *77* (17), 2127–2140.

(12) Sehar, I.; Kaul, A.; Bani, S.; Pal, H. C.; Saxena, A. K. Immune up regulatory response of a non-caloric natural sweetener, stevioside. *Chem.-Biol. Interact.* **2008**, *173* (2), 115–121.

(13) Carakostas, M.; Curry, L.; Boileau, A.; Brusick, D. Overview: The history, technical function and safety of rebaudioside A, a naturally occurring steviol glycoside, for use in food and beverages. *Food Chem. Toxicol.* **2008**, *46* (7), S1–S10.

(14) Jaitak, V.; Kaul, V. K.; Bandna; Kumar, N.; Singh, B.; Savergave, L. S.; Jogdand, V. V.; Nene, S. Simple and efficient enzymatic transglycosylation of stevioside by β-cyclodextrin glucanotransferase from *Bacillus Firmus*. *Biotechnol. Lett.* **2009**, *31* (9), 1415–1420.

(15) Maki, K. C.; Curry, L. L.; Carakostas, M. C.; Tarka, S. M.; Reeves, M. S.; Farmer, M. V.; McKenney, J. M.; Toth, P. D.; Schwartz, S. L.; Lubin, B. C.; Dicklin, M. R.; Boileau, A. C.; Bisognano, J. D. The hemodynamic effects of rebaudioside A in healthy adults with normal and low-normal blood pressure. *Food Chem. Toxicol.* **2008**, *46* (7, Suppl. 1), S40–S46.

(16) Williams, L. D.; Burdock, G. A. Genotoxicity studies on a high-purity rebaudioside A preparation. *Food Chem. Toxicol.* **2009**, *47* (8), 1831–1836.

(17) Roberts, A.; Renwick, A. G. Comparative toxicokinetics and metabolism of rebaudioside A, stevioside, and steviol in rats. *Food Chem. Toxicol.* **2008**, *46* (7, Suppl. 1), S31–S39.

(18) Curry, L. L.; Roberts, A.; Brown, N. Rebaudioside A: Two-generation reproductive toxicity study in rats. *Food Chem. Toxicol.* **2008**, *46* (7, Suppl. 1), S21–S30.

(19) Renwick, A. G. The use of a sweetener substitution method to predict dietary exposures for the intense sweetener rebaudioside A. *Food Chem. Toxicol.* **2008**, *46* (7, Suppl. 1), S61–S69.

(20) Gardana, C.; Simonetti, P.; Canzi, E.; Zanchi, R.; Pietta, P. Metabolism of Stevioside and Rebaudioside A from *Stevia rebaudiana* Extracts by Human Microflora. *J. Agric. Food Chem.* **2003**, *51* (22), 6618–6622.

(21) Jackson, M. C.; Francis, G. J.; Chase, R. G. High yield method of producing pure Rebaudioside A. U.S. patent application, 2006-0083838Al.

(22) Evans, J. C.; Hahn, J. J.; Myerson, A. S.; Oolman, T.; Rhonemus, T. A.; Storo, K. M.; Tyler, C. A. Method of producing purified Rebaudioside A compositions using solvent/antisolvent crystallization. U.S. patent application, 20100099857Al.

(23) Abelyan, V.; Markosyan, A.; Abelyan, L. Process for manufacturing a sweetenerand use thereof. U.S. patent application, 2010-0112154Al.

(24) Purkayastha, S.; Markos, A.; Malsagov, M. Process for manufacturing a sweetenerand use thereof. U.S. patent application, 2010-0255171Al.

(25) Guo, M.; Liang, J.; Wu, S. On-line coupling of counter-current chromatography and macroporous resin chromatography for continuous isolation of arctiin from the fruit of *Arctium lappa L. J. Chromatogr. A* **2010**, *1217* (33), 5398–5406.

(26) Scordino, M.; Di Mauro, A.; Passerini, A.; Maccarone, E. Adsorption of Flavonoids on Resins: Hesperidin. *J. Agric. Food Chem.* **2003**, *51* (24), 6998–7004.

(27) Scordino, M.; Di Mauro, A.; Passerini, A.; Maccarone, E. Adsorption of Flavonoids on Resins: Cyanidin 3-Glucoside. *J. Agric. Food Chem.* **2004**, *52* (7), 1965–1972.

(28) Liu, Y.; Liu, J.; Chen, X.; Liu, Y.; Di, D. Preparative separation and purification of lycopene from tomato skins extracts by macroporous adsorption resins. *Food Chem.* **2010**, *123* (4), 1027–1034.

(29) Chen, Z.; Liu, Y.; Huang, X.; Fu, J.; Di, D. The Separation of Steviosides in the leaves of *Stevia rebaudiana* Bertoni by Macroporous Resin. *J. Polym. Mater.* **2011**, *28* (1), 75–92.

(30) Cabanne, C.; Pezzini, J.; Joucla, G.; Hocquellet, A.; Barbot, C.; Garbay, B.; Santarelli, X. Efficient purification of recombinant proteins fused to maltose-binding protein by mixed-mode chromatography. *J. Chromatogr. A* **2009**, *1216* (20), 4451–4456.

(31) Voitl, A.; Müller-Späth, T.; Morbidelli, M. Application of mixed mode resins for the purification of antibodies. *J. Chromatogr. A* **2010**, *1217* (37), 5753–5760.

(32) Chen, J.; Tetrault, J.; Zhang, Y.; Wasserman, A.; Conley, G.; DiLeo, M.; Haimes, E.; Nixon, A. E.; Ley, A. The distinctive separation attributes of mixed-mode resins and their application in monoclonal antibody downstream purification process. *J. Chromatogr. A* **2010**, *1217* (2), 216–224.

(33) Chen, Z.; Zhang, A.; Li, J.; Dong, F.; Di, D.; Wu, Y. Study on the Adsorption Feature of Rutin Aqueous Solution on Macroporous Adsorption Resins. *J. Phys. Chem. B* **2010**, *114* (14), 4841–4853.

(34) Huang, X. Y.; Fu, J. F.; Di, D. L. Preparative isolation and purification of steviol glycosides from *Stevia rebaudiana* Bertoni using high-speed counter-current chromatography. *Sep. Purif. Technol.* **2010**, *71* (2), 220–224.

(35) Liu, J.; Li, J. W.; Tang, J. Ultrasonically assisted extraction of total carbohydrates from *Stevia rebaudiana* Bertoni and identification of extracts. *Food Bioprod. Process.* **2010**, *88* (2−3), 215–221.

(36) Ho, Y. S.; McKay, G. Sorption of dye from aqueous solution by peat. *Chem. Eng. J.* **1998**, *70* (2), 115–124.

(37) Dizge, N.; Keskinler, B.; Barlas, H. Sorption of Ni(II) ions from aqueous solution by Lewatit cation-exchange resin. *J. Hazard. Mater.* **2009**, *167* (1−3), 915–926.

(38) Zhang, Z.; Xu, X.; Yan, Y. Kinetic and thermodynamic analysis of selective adsorption of Cs(I) by a novel surface whisker-supported ion-imprinted polymer. *Desalination* **2010**, *263* (1−3), 97–106.

(39) Tan, I. A. W.; Ahmad, A. L.; Hameed, B. H. Adsorption of basic dye on high-surface-area activated carbon prepared from coconut husk: Equilibrium, kinetic and thermodynamic studies. *J. Hazard. Mater.* **2008**, *154* (1−3), 337–346.

(40) Ma, C.; Tao, G.; Tang, J.; Lou, Z.; Wang, H.; Gu, X.; Hu, L.; Yin, M. Preparative separation and purification of rosavin in Rhodiola rosea by macroporous adsorption resins. *Sep. Purif. Technol.* **2009**, *69* (1), 22–28.